

Study of 22/20nm Tri-Gate Transistors Compatible in a Low-Cost Hybrid FinFET/Planar CMOS Process

T. Baldauf^a, A. Wei^b, R. Illgen^b, S. Flachowsky^b, T. Herrmann^b
J. Höntschel^b, M. Horstmann^b, W. Klix^a, and R. Stenzel^a

^a Department of Electrical Engineering, University of Applied Sciences Dresden, Germany,
tim.baldauf@htw-dresden.de

^b GLOBALFOUNDRIES Dresden Module One LLC & Co.KG, Germany

Introduction: For future scaling to the end of the ITRS roadmap, novel structures like FinFETs are required to improve electrostatic integrity of MOSFETs with gate lengths shorter than 35 nm [1-4]. Classic fully-depleted FinFETs with a high aspect ratio are not compatible with existing planar process flows. A Tri-Gate transistor has the advantage of being more compatible. It is even possible to produce low-profile Tri-Gates in parallel to planar MOSFETs [5], with shared Tri-Gate and planar implants and common-use of source/drain epi and dual band-edge metal gate workfunctions. This maintains the design flow, saves mask count, allows reuse of analog and high-voltage I/O designs, while exploiting Tri-Gates in high speed logic and low minimum voltage.

Results and Discussion: To demonstrate this concept, a planar CMOS process was first simulated in 3-D around 22 nm technology ground rules with an assumed nominal $L_{\text{gate}} = 26$ nm and $EOT = 1.0$ nm, in line with ITRS assumptions. The planar MOSFET 3-D process simulation was then extended by an additional mask, etch, and deposition step to create a Tri-Gate structure, as shown in Fig.1. Following the fin formation, planar and Tri-Gate MOSFETs are running the same process in terms of implants and epitaxial S/D. The resulting dopant profiles in the Tri-Gate transistor are nearly identical to that of the planar process. Tri-Gate transistors with 20nm fin width and 10nm high side gates have significantly better gate control and show significant improvement of DIBL and subthreshold slope (sat.) from 92 mV/dec to 73 mV/dec (NMOS, Fig.2) and from 95 mV/dec to 77 mV/dec (PMOS). This translates into an effective EOT reduction in the Tri-Gates, and thus effectively reduces random doping fluctuation (RDF). Due to the improved electrostatics of the low-profile halo-doped Tri-Gate, halo dose to be further reduced while maintaining subthreshold slope as shown in Fig. 3, for additional improvement in RDF. This improvement in electrostatics can translate into L_{gate} scaling as well. The significance of the enhanced electrostatic behavior of Tri-Gates is further illustrated in Fig. 4. Planar MOSFETs show a clear V_T -rolloff to sub-nominal while Tri-Gate rolloff curves remain almost flat.

The low-profile halo-doped Tri-Gate exhibits a lower threshold voltage caused by improved subthreshold slope and a high electron density at the corners due to corner effects [6]. There are two relevant solutions to suppress corner effects and for retargeting of Tri-Gate threshold voltage. The first is a corner rounding process, which is already induced by process cleaning steps. Another solution requires an additional corner implantation which is self-aligned to Tri-Gate corner regions via fin formation nitride hardmask, and allows a homogenous counter doping over the whole gate length.

Optimization of fin geometry is studied by a variation of fin height (0 - 50 nm) and width (15 - 30 nm). Starting from the planar limit, segmentation of the active area into W_{Fin} and addition of gate wrap-around with H_{Fin} , the subthreshold slope decrease and shows a saturation at $H_{\text{Fin}} = 10$ nm.

With a planar-like extension/halo dopant profile, higher fins have also a worse behavior of $I_{D,\text{off}}$ and $I_{D,\text{sat}}$ due to series resistance. Fig. 5 demonstrates that a fin height of 7 nm and width of 20 nm is the optimal Tri-Gate geometry, where 7nm matches the extension junction depth. A narrow fin less than 15 nm becomes fully-depleted and is not useful for a hybrid CMOS process as it requires another gate metal workfunction to maintain positive V_T , and is thus no longer compatible with co-processed planar transistors. The stability of threshold voltage and subthreshold slope depending on process variations (H_{Fin} or $W_{\text{Fin}} \pm 4$ nm) is shown by Fig. 6. H_{Fin} is the most critical parameter and must be very well controlled in process.

Conclusion: A low-profile extension/halo-doped Tri-Gate which is compatible to a planar process has been evaluated and shows significant electrostatic and drive current benefits compared to planar. This is maintained over a large design space of Tri-Gate fin width and height. Such a Tri-Gate is the basis for a

low-cost Tri-Gate/planar hybrid technology, where Tri-Gates and planar would share the same implant masking, same S/D processes, and same dual band-edge metal gate workfunctions. In such a technology, planar transistors could be run at longer channel lengths to support analog and high voltage I/O, while Tri-Gates would be run in low-voltage SRAM and high speed logic.

References:

[1] P. Packan et al. "High performance 32nm logic technology featuring...", IEDM Tech. Dig. 2009 pp.659-662
 [2] A. Tilke et al. "Mikroelektronik: kein Ende der Skalierung in Sicht", Physik Journal Nr.6 2007, pp. 35-41
 [3] K. Okano et al. "Process Integration Technology and Device Charact...", IEDM Tech. Dig. 2005, pp. 721-724
 [4] C.Y. Chang et al. "A 25-nm Gate-Length FinFET Transistor Module for...", IEDM Tech. Dig. 2009, pp. 293-296
 [5] X. Sun et al. "Tri-Gate Bulk MOSFET...", IEEE Electron Device Letters, vol. 29, no. 5, pp. 491-493, May 2009
 [6] B. Doyle et al. "Tri-Gate Fully-Depleted CMOS Trans...", VLSI, Dig. of Tech. Papers, pp. 133-134, June 2003

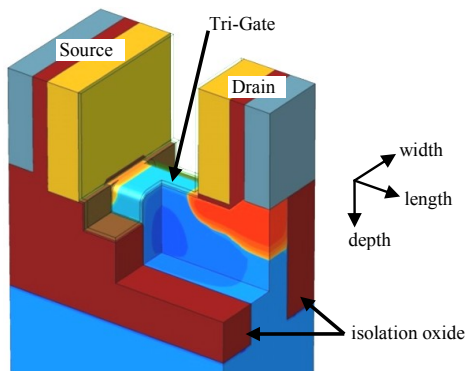


Fig. 1: Simulated n-Tri-Gate transistor cut at the half-Tri-Gate transistor width and length.

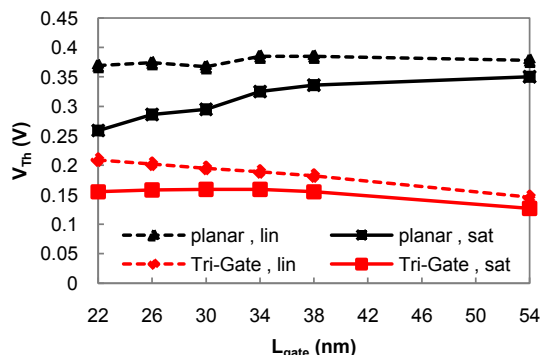


Fig. 4: Simulated roll-off curve for a planar and Tri-Gate NMOS ($H_{Fin} = 10\text{nm}$, $W_{Fin} = 20\text{nm}$)

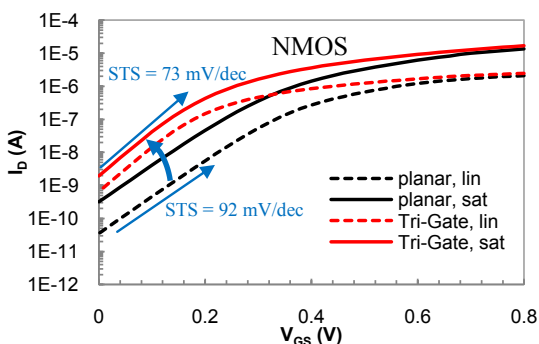


Fig. 2: Transfer characteristic (log.) for a planar and Tri-Gate NMOS ($H_{Fin} = 10\text{nm}$, $W_{Fin} = 20\text{nm}$, $L_{gate} = 26\text{nm}$)

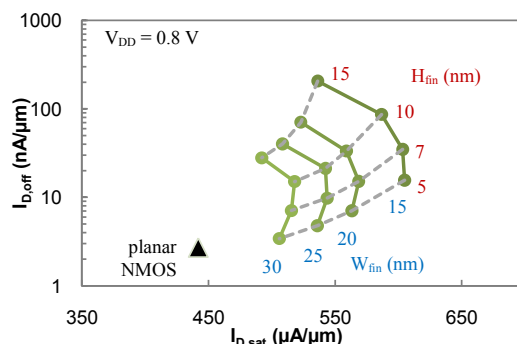


Fig. 5: $I_{D,off}$ to $I_{D,sat}$ normalized to total gate width for different widths and heights of Tri-Gate NMOS ($L_{gate} = 26\text{nm}$)

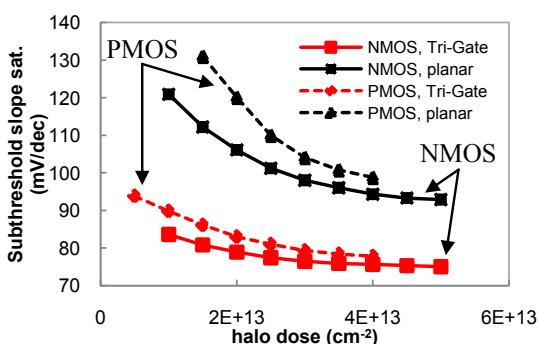


Fig. 3: Subthreshold slope of planar and Tri-Gate N- and PMOS as a function of halo dose ($L_{gate} = 26\text{nm}$)

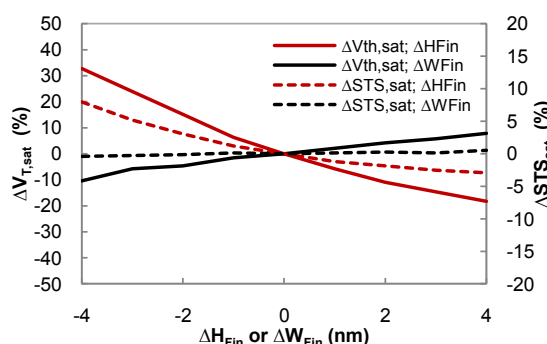


Fig. 6: Percent change of NMOS threshold voltage and subthreshold slope depending of ΔH_{Fin} or ΔW_{Fin} . Note that PMOS looks similar. ($H_{Fin} = 10\text{nm}$, $W_{Fin} = 20\text{nm}$, $L_{gate} = 26\text{nm}$)